



Low temperature Synthesis of Zinc Oxide nanoparticles and their characterization

¹Muhammed Shajudheen V P, ²Anitha Rani K, ³Senthil Kumar V, ⁴Sivakumar M and ⁵Saravana Kumar S

^{1,2,3}Department of Physics, Karpagam University, Coimbatore, Tamil Nadu, India

⁴Department of Sciences, Amrita Vishwa Vidya Peetham, Coimbatore, Tamil Nadu, India

⁵Department of Physics, NSS College Pandalam, Kerala, India

Email: shajuvp099@gmail.com

Abstract: We report, a simple and low cost chemical precipitation method adopted to prepare zinc oxide nanoparticles (ZnO) using polyvinyl pyrrolidone (PVP) as a capping agent. The thermal, structural, morphological and optical properties have been characterized by different techniques such as DSC-TGA, X-Ray Diffraction (XRD), Micro Raman spectroscopy, Fourier Transform Infra-Red spectroscopy (FTIR), Field Effect Scanning Electron Microscopy (FESEM), UV-Visible absorption spectroscopy (UV-Vis) and Photoluminescence spectroscopy (PL). From, DSC-TGA result, above 900°C it become stable with no further weight loss is obtained. X-ray diffraction results confirmed the wurtzite hexagonal structure of ZnO nanoparticles. The two intensive peaks at 162 and 432 cm^{-1} in the Raman Spectrum are attributed to the first order modes of the wurtzite ZnO nanoparticles. The mixed shapes of grapes, sphere, hexagonal and rocks like structures have been noticed in FESEM. The band gap obtained from the UV-Vis absorption spectra, shows a blue shift, which is attributed to increase in carrier concentration (Burstein Moss Effect). Photoluminescence studies of the single crystalline ZnO nanoparticles show a strong peak centered at 385 nm, corresponding to the near band edge emission in ultraviolet range.

Keywords: ZnO nanoparticles, simple chemical precipitation route, mixed shape morphology

I. INTRODUCTION

In recent years, there was grown in interest to synthesis nanoparticles, which have been different from bulk materials by a reduction in volume and an increase in the specific surface area [1-4]. Nanoparticles of ZnO have been drawn great interest in research due to their unique electronic, optical, mechanical, magnetic and chemical properties and have broad attention due to its wide range of applications in ultraviolet (UV) lasers, power generators, solar cells, gas sensors, field emission devices, capacitors, transparent UV resistance coating, electrochemical and electromechanical nanodevices, sun screen lotion (cream), cosmetic and medicated creams etc [5-14]. Several physical and chemical methods have been developed to obtain ZnO nanoparticles which include, reverse micelles process, solid state reaction,

sol-gel method, ultrasonic irradiation, combustion method, solvothermal synthesis, electrochemical synthesis and chemical precipitation method etc [15-24].

We report a simple low temperature method to synthesize ZnO nanoparticles. The samples were characterized using X-Ray Diffraction (XRD), Micro Raman spectroscopy, UV-Visible absorption spectroscopy (UV-Vis), Fourier Transform Infra-Red spectroscopy (FTIR), Photoluminescence spectroscopy (PL) and Field Effect Scanning Electron Microscopy (FESEM).

II. EXPERIMENTAL

All the chemicals reagents used in our experiments were of analytical grade, commercially purchased from Merck used as received without further purification. 250ml deionized water is taken in a beaker and 0.05gm PVP is added. The solution is stirred 10 minutes using magnetic stirrer and then added 22.43 gm of $\text{ZnSO}_4 \cdot \text{H}_2\text{O}$ to the solution and stirred continuously for 2 hours. To this solution 15.5ml of 2M NH_4OH added dropwise while the reactants are continuously stirred till the pH becomes 5.5. After 1hour reflexing the precipitate formed is centrifuged, washed several times with water and finally with ethanol, and then air dried to obtain nano powders of zinc hydroxide. The oxidation mechanism of zinc hydroxide from ambient temperature upto 1000°C was investigated by thermogravimetric (TG) and Differential scanning calorimeter (DSC) using Perkin Elmer, Diamond DSC-TGA set up.

X-ray Diffraction patterns of the zinc oxide sample were recorded using a Philips Xpert pro Diffractometer and using $\text{CuK}\alpha$ radiation over the diffraction angles (2θ) from 30 to 80°.

The micro Raman spectra of ZnO nanoparticles were recorded using Horiba Labram-HR, in the range of 100-1500 cm^{-1} . The Nd:YAG laser operating at 200mW, 150nm as the excitation wavelength, and a liquid nitrogen cooled Ge detector was used to record the spectrum. The room temperature FT-IR spectrum of ZnO nanoparticles was recorded in the range of 400-

4000 cm^{-1} , using Shimadzu FTIR-8400S spectrometer, using KBr pellet technique. The Field Effect Scanning Electron Microscope images of titanium oxide nanoparticles were recorded using Carl Zeiss Sigma HD FESEM. UV-Vis absorption spectrum and photoluminescence spectrum of nanoparticles of ZnO were recorded using Varian, Cary 5000 spectrophotometer and JASCO FP 8200 Spectrofluorometer.

III. RESULTS AND DISCUSSION

3.1 Thermogravimetric Analysis

Figure 1 shows the differential scanning calorimeter (DSC) and thermogravimetric analysis (TGA) curve of as prepared zinc hydroxide nanopowders. The thermal analysis was carried out in the temperature range of 10°C–1000°C, to find the decomposition and phase formation that occurs during heat treatment of the as-prepared compound of zinc hydroxide nanoparticles.

Two consecutive steps can be observed within the temperature ranges 10°C–400°C and 410°C–820°C corresponding to weight loss can be observed in the DSC-TGA curves. The first step corresponding to mass loss (21.06%) can be attributed to the removal of water and other hydroxyl groups. A slow decay corresponding to mass loss (10.82%) observed at 410°C–900°C can be attributed to the loss of NH_4OH and other organic species present in the sample. Above 900°C it becomes stable with no further weight loss. Based on these results, the ZnOH samples of present study were annealed at 1000°C.

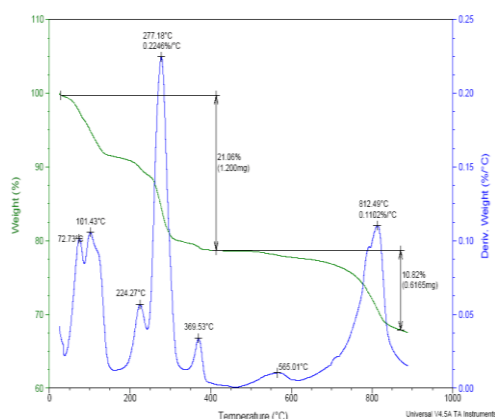


Fig.1 DSC-TGA curves of ZnO nanoparticles

3.2 X-Ray Diffraction Studies

The X-ray diffraction (XRD) pattern recorded in the range of 30° to 80° with $\text{CuK}\alpha$ radiation of prepared ZnO nanoparticles is shown in Fig.2. The prominent peaks existed at an angle of $2\theta = 31.73^\circ, 34.36^\circ, 36.21^\circ, 47.46^\circ, 56.52^\circ, 62.75^\circ, 67.85^\circ, 68.99^\circ, 72.43^\circ$ and 76.84° corresponding to the planes of (100), (002), (101), (102), (110), (103), (200), (112), (201), (004) and (202) of hexagonal (wurtzite) phase of ZnO [80–0074, JCPDS]. Similar results have been observed by literatures [25–27]. Using XRD data the grain size and

the lattice constant has been calculated. The average crystallite size, estimated by Debye-Scherrer formula, the particle size (D) can be calculated as, $D = 0.9\lambda/\beta\cos\theta$, where λ is the X-ray wavelength (1.54060 Å), β is the full width at half maximum (FWHM), 0.9 is the Scherrer constant and θ is the Bragg's angle for the (100), (002), and (101) diffraction peaks are found to be 32 nm. From XRD data, the lattice constants were determined to be $a=3.253$ and $c=2.851$ nm and its space group: P63mc.

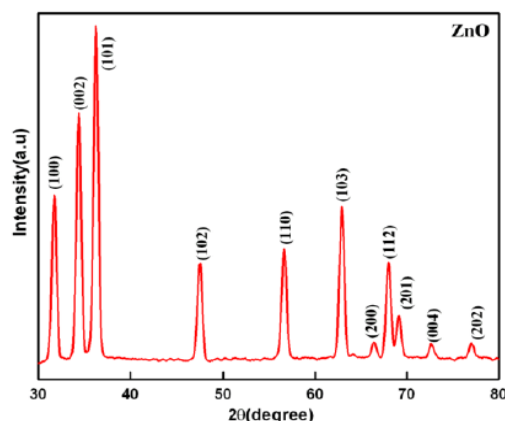


Fig.2 XRD pattern of ZnO nanoparticles

3.3 Micro Raman Studies

The micro Raman spectrum of nanoparticles of ZnO is shown in figure 3. The spectrum shows intense peak at 162, 251, 432 and 1120 cm^{-1} . The peak at 162 cm^{-1} can be attributed to plasma from excitation source. The peak at 432 cm^{-1} can be attributed to E_2 (high) mode of wurtzite ZnO. The presence of E_2 (high) mode which is a characteristic peak of ZnO in the Raman spectrum of present sample matches well with the XRD results. The peak at 1120 cm^{-1} can be attributed to $2E_1(\text{LO})$ mode of ZnO. The peak at 251 cm^{-1} does not correspond to first or second order modes of wurtzite ZnO. This peak may be attributed to anomalous Raman modes in ZnO due to the presence of large number of defects. Several authors reported the observation of anomalous modes in Raman spectra of bulk ZnO [28–30].

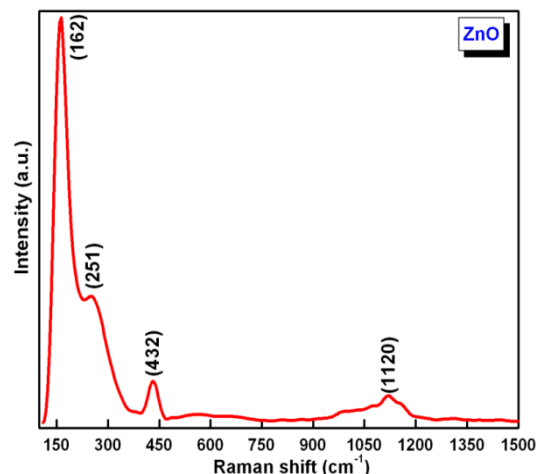


Fig.3 Micro-Raman spectrum of ZnO nanoparticles

3.4 FTIR Studies

Figure 4 shows the FTIR absorption spectrum of the samples of present study. The absorption peak corresponding to the Zn-O bonds above 442 cm^{-1} can be observed. The peak at 3446 cm^{-1} can be attributed to the presence of symmetric and asymmetric vibrations of -OH (hydroxyl groups) and C=O groups, probably due to the atmospheric moisture and molecules of CO_2 respectively. The absorption bands at $1050\text{--}1650\text{ cm}^{-1}$ and above 440 cm^{-1} implies the presence of stretching vibrations of the CO-Zn and the -OH group on the surface of ZnO nanoparticles [31].

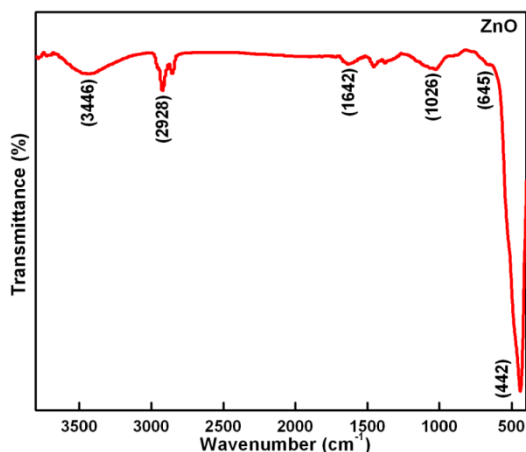


Fig.4 FTIR spectra of ZnO nanoparticles

3.5 Field Effect Scanning Electron Microscope Studies

Field Effect Scanning Electron Microscopy (FESEM) is used to study the deposition of expected nanoparticles on its surface. The FESEM images of the prepared ZnO nanoparticles are shown in Figure 5. Surface properties directly affect the optical properties of the films. From the FESEM analysis, it can be observed that the distributions of grains are not consistent throughout all the regions. The graphs-like structure in the FESEM clearly indicates the mixed shape of sphere, hexagonal, rod with small voids, rock like structure and spongy like structure.

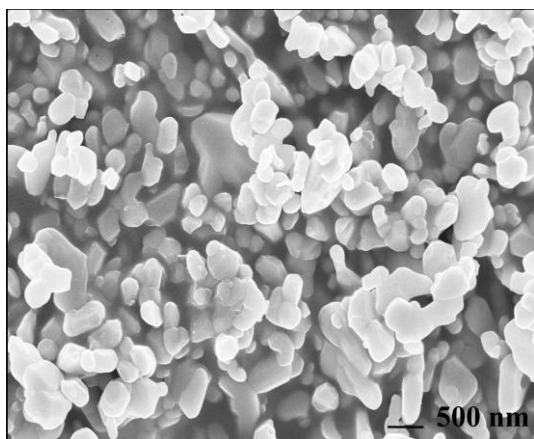


Fig.5 FESEM micrographs of ZnO nanoparticles

3.6 UV-Visible Absorption Studies

The reflection and absorption spectra of the ZnO nanoparticles as function of wavelength are shown in the Fig.6 and fig.7 respectively. It can be observed from the absorption spectrum that the absorption edge is shifted to higher wavelengths. This can be ascribed to the smaller particle size of the ZnO nanoparticles. This can be assigned to the intrinsic band gap absorption of ZnO due to the electron transitions from the valence band to the conduction band [32].

The optical band gap energy (E_g) can be estimated from absorption coefficient (α) using the Tauc relation:

$$\alpha h\nu = A(h\nu - E_g)^q$$

where A is a constant that depends on the transition probability, $h\nu$ is the energy of an incident photon, and q is an index that characterizes the optical absorption process. It is well known that direct and indirect band gap energy for the semiconductor nanostructures can be obtained from the intersection of linear fits of $(\alpha h\nu)^{1/q}$ versus $h\nu$ plots for $q=1/2$ and 2 on the x-axis[33]. ZnO is the direct bandgap semiconductor material, so we can choose $q=1/2$ in the estimation. Fig.8, shows the plot of $(\alpha h\nu)^2$ vs $h\nu$ for ZnO nanoparticles. The band gap calculated from the plot is 3.1eV

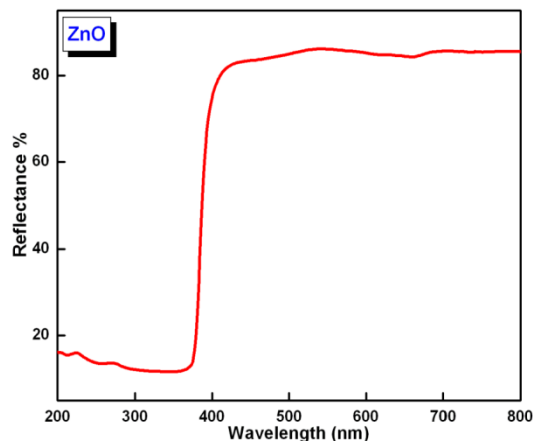


Fig.6 Reflection spectrum of ZnO nanoparticles

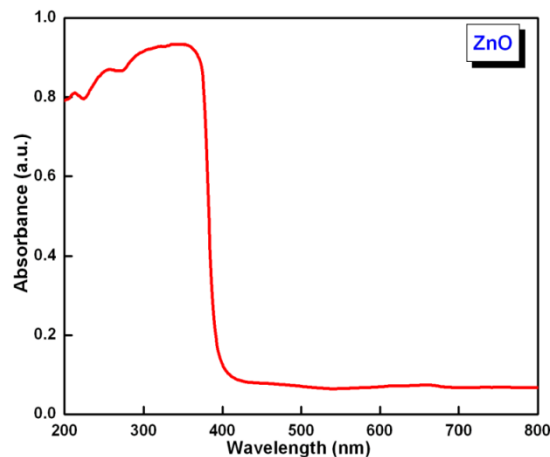


Fig.7 UV absorption spectra of ZnO nanoparticles

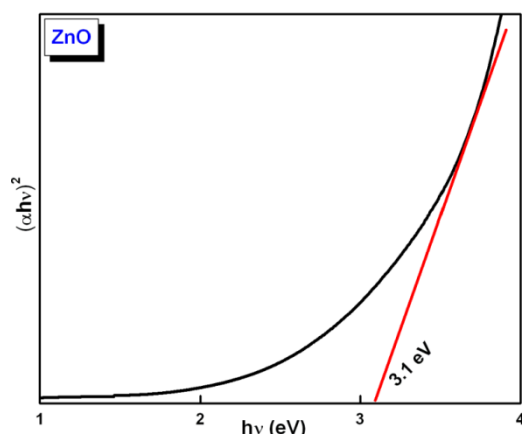


Fig.8 Band gap of ZnO nanoparticles

3.7 Photoluminescence Studies

Fig.9 shows the room-temperature photoluminescence spectrum of the ZnO nanoparticles. The prepared ZnO nanoparticles exhibited both excitonic emission band in the range at 385 nm and the broad green band in the range at 505 nm. And it confirms that ZnO nanoparticles covered both UV regions to whole of the visible region. The presence of visible green emission is due to its zinc vacancy, oxygen vacancy, oxygen interstitial and antisite oxygen [34, 35]. A large number of oxygen vacancies are occurred due to their nanosized particles in a large surface-to-volume ratio. The presence of green emission peak in the photoluminescence spectrum of samples of present study may be attributed to photon induced charge transfer transition state.

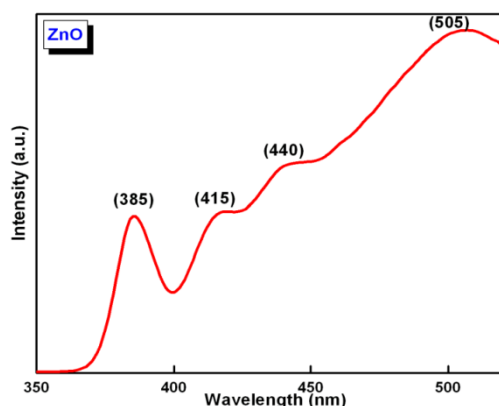


Fig.9 Photoluminescence spectrum of ZnO nanoparticles

IV. CONCLUSION

Using simple chemical precipitation method, we have synthesized ZnO nanoparticles. The two mass loss steps of TG curve in the temperature ranges 10°C–400°C and 410°C–820°C can be attributed to loss of hydroxyl group and NH₄OH respectively. From the XRD pattern, it was observed that the samples of the present study are in wurtzite phase of ZnO. The grain size calculated from XRD is approximately 32nm. The band gap calculated from UV-Visible absorption spectrum is 3.1eV. The photoluminescence spectrum of the ZnO nanoparticles

of the present study exhibited excitonic emission band at 385 nm and the broad green band at 505 nm.

REFERENCES

- [1] Maciej Mazur, *Electrochemistry Communications* 6 (2004) 400-403.
- [2] Lili Feng, Chunlei Zhang, Guo Gao, Daxiang Cui, *Nanoscale Research Letters* 7 (2012) 1-10.
- [3] Angshuman Pal, Sunil Shah, Surekha Devi, *Colloids and Surfaces A Physicochemical and Engineering Aspects* 302 (2007) 483-487.
- [4] M. J. Rosemary, Thalappil Pradeep, *Colloids and Surfaces A Physicochemical and Engineering Aspects A* 268 (2003) 81-84.
- [5] Yingwei Xie, Ruqiang Ye, Honglai Liu, *Colloids and Surfaces A Physicochemical and Engineering Aspects* 279 (2006) 175-178.
- [6] Michael H. Huang, Samuel Mao, Henning Feick, Haoquan Yan, Yiyang Wu, Hannes Kind, Eicke Weber, Richard Russo, Peidong Yang, *Science* 292 (2001) 1897-1899.
- [7] Xudong Wang, Jinhui Song, Jin Liu, Zhang L. Wang, *Science* 316 (2007) 102-105.
- [8] C. Y. Jiang, X. W. Sun, G. Q. Lo, D. L. Kwong, J. X. Wang, *Applied Physics Letters* 90 (2007) 263501-263503.
- [9] Qing Wan, Q. H. Li, Y. J. Chen, Ta-Hung Wang, X. L. He, J. P. Li, C. L. Lin, *Applied Physics Letters* 84 (2004) 3654-3656.
- [10] Chia Ying Lee, Seu Yi Li, Pang Lin, Tseung-Yuen Tseng, *Journal of Nanoscience Nanotechnology* 5 (2005) 1088-1094.
- [11] Hung-Ta Wang, B. S. Kang, Fan Ren, L. C. Tien, P. W. Sadik, D. P. Norton, S. J. Pearton, J. Lin, *Applied Physics Letters* 86 (2005) 243503-243505.
- [12] Jih-Jen Wu, Guan-Ren Chen, Hung-Hsien Yang, Chen-Hao Ku, Jr-Yuan Lai, *Applied Physics Letters* 90 (2007) 213109-213111.
- [13] S. F. Yu, C. Yuen, S. P. Lau, W. I. Park, G. C. Yi, *Applied Physics Letters* 84 (2004) 3241-3243.
- [14] Nick Serpone, Deniele Dondi, Angelo Albini, *Inorganica Chimica Acta* 360 (2007) 794-802.
- [15] Surabhi S. Kumar, Putcha Venkateswarlu, Vanka. R. Rao, Gollapalli N. Rao, *International Nano Letters* 3 (2013) 1-6.
- [16] M. Maillard, S. Giorgio, Marie P. Pileni, *Advanced Material* 14 (2002) 1084-1086.
- [17] Zeena S. Pillai, Prashant V. Kamat, *The Journal of Physical Chemistry B* 108 (2004) 945-951.

- [18] Kirti Patel, Sudhir Kapoor, D. P. Dave, Tulsi Murherjee, *Journal of Chemical Science* 117 (2005) 53-60.
- [19] R. A. Salkar, P. Jeevanandam, S. T. Aruna, Yuri Koltypin, A. Gedanken, *Journal of Materials Chemistry* 9 (1999) 1333-1335.
- [20] Behrouz Soroushian, Isabelle Lampre, Jacqueline Belloni, Mehran Mostafavi, *Radiation Physics Chemistry* 72 (2005) 111-118.
- [21] B. G. Ershov, E. Janata, A. Henglein, A. Fojtik, Unpublisch report (2007).
- [22] Maria Starowicz, Barbara Stypula, Jacek Banaoe, *Electrochemistry Communications* 8 (2006) 227-230.
- [23] Jun-Jie Zhu, Xue-Hong Liao, Xiao-Ning Zhao, Hong-Yuang Hen, *Material Letters* 49 (2001) 91-95.
- [24] S. Liu, S. Chen, S. Avivi, A. Gendanken, *Journal of Non-crystalline Solids* 283 (2001) 231-236.
- [25] X. Y. Li, Y. Hou, Q. D. Zhao and L. Z. Wang, *J. Colloid Interf. Sci.*, 358, 102-108, 2011.
- [26] M.K. Patra, K. Manzoor, M. Manoth, S.R. Vadera, N. Kumar, *J. Lumin.* 128(2008) 267.
- [27] T. Sun, J. Qiu, Ch. Liang, *J. Phys. Chem. C* 112 (2008) 715.
- [28] F J Manjon, B.Mari, J.Serrano and AH Romero Vol. 97, (2005), *J.Appl.Phys.*053516.
- [29] M Tzolov, N.Tzenov, D.Dimova-Malinovska, M.Kalitzova, C.Pizzuto, G.Vitali, G.Zollo, and I. Ivanov, *Thin Solid Films* 379, 28 (2000); 396274 (2001).
- [30] X.Q.Wang, S.Yang, J.Wang, M.Li, X.Jiang, G.Du, X.Liu, and R.P.H. Chang , *J. Cryst. Growth* 226,123(2001).
- [31] A.Kaschner et al.,*Appl.Phys.Lett.*80,1909(2002).
- [32] Y.G.Wang, S.P. Lau, X.H. Zhang, H.W. Lee, H.H. Hng, and B.K. Tay, *J Cryst. Growth* 252, 265 (2003).
- [33] C.Bundesmann, N.Ashkenov, M.Schubert, D. Spemann, T.Butz, E.M. Kaidashev, M.Lorenz, and M. Grundmann, *Appl. Phys. Lett.*83, 1974(2003).
- [34] F.Reuss, C.Kirchner, Th.Gruber, R.Kling, S.Maschek, W.Limmer, A.Waag, and P.Ziemann, *J. Appl. Phys.* 95, 3385 (2004).
- [35] Wehner PS, Mercer PN, Apai G: Interaction of H₂ and CO with Rh₄(CO)₁₂ supported on ZnO. *J Catal* 1983, 84:244–247.

